Contemporary Mathematics
http://ojs.wiserpub.com/index.php/CM/

Research Article

A Multi Objective Solution to Integrated Power System in the Presence of Thyristor Controlled Series Compensator

MD. Yaseen*, **Sravana Kumar Bali**[1]

EEE Department, GITAM Deemed to be University, Visakhapatnam, Andhra Pradesh, India
E-mail: yaseen.eee08@gmail.com

Received: 21 November 2023; **Revised:** 4 December 2023; **Accepted:** 29 March 2024

Abstract: The current geopolitical climate has highlighted the significance of maximizing the world's energy potential. The optimal use of available assets lowers the cost of electricity to customers. This study proposes a multi-objective ideal power flow for a composite transmission network with FACTS devices. The multi-objective function used in this work is a novel approach. Objectives include minimizing voltage variance, power loss, and negative social welfare (NSW). A Thyristor Controlled Series Compensator (TCSC) FACTS device is employed in this work to test on IEEE 57 bus system. Moth Flame Optimization Algorithm maximized the objective function. The results are detailed, compared, and assessed.

Keywords: FACTS devices, moth flame optimization algorithm, optimal power flow

MSC: 76Z05, 92C10, 92C35

1. Introduction

India has a large population and growing electrical demand. Since power deregulation, transmission corridor pressure has increased. The power business now prioritizes power flow optimization. The only way to match HVDC systems' efficiency without breaking the bank is to use FACTS devices in the AC transmission system. Congestion limits were addressed by Lawal et al. [1] for optimal hydro-thermal power flow. Power flow tracking may identify the generators causing crowded lines and increase their output. Establishing a penalty number for the maximum power of the affected generators reduces congestion. Batra et al. [2] used the TECM-PSO algorithm (TECM) to non-linear congestion management in a deregulated energy system to improve twin extremity mapping of the chaotic map. The hybrid PSO-APO algorithm by Teeparthi et al. [3] considers wind and heat generators for emergencies.

Power system difficulties have been solved via FACTS devices [4]. Visakha et al. [5] devised a plan to deploy a UPFC in a suitable place while anticipating problems. Nusair et al. [6] optimized a renewable-system power system utilizing TCSC. For cost savings, authors employed OPF with FACTS devices [7]. Authors conducted OPF for an integrated wind farm system using TCSC and UPFC to minimize costs [8]. Managing power system issues requires proper FACTS device deployment and adjustment. IPFC has solved power system congestion and contingency issues [9, 10]. Due of IPFC's multiple connections, placement must be considered [11]. Voltage index-based contingency analysis is suggested in [12]. Kumar et al. [13] suggest IPFC placement using cat swarm optimization to increase voltage stability. Verma et al. [14]

DOI: https://doi.org/10.37256/cm.5320243978

advised placing FACTS devices there for voltage stability. Research has examined power grid FACTS device regulation [15, 16]. As advocated in [17], placing and sizing FACTS devices for greatest social welfare may decrease load shedding and branch costs and increase the public benefit. Optimizing public good activities seems natural. [18, 19] shown that optimal power flow and FACTS location and size may achieve multi-objective functions.

This study proposes a multi-objective OPF for an integrated power system. Traditional generators, solar array, and wind turbine comprise the transmission network. Losses voltage deviation reduction and welfare improvement are optimization's main aims. A negative social welfare was created to fit the objective function as it is a minimization function. There were three stages to the completion of the goals. First, an OPF for the MOP has been run on the whole system integration. The ideal location of TCSC in the power system has then been determined using an index. The TCSC is now set up to maximize future success in reaching the goals. At long last, the integrated system has been fine-tuned once again to achieve its goals. The system's resilience has been evaluated using a contingency analysis. The findings have been presented and examined, and they highlight the system's resilience when subjected to erratic inputs. The research makes use of a bus system based on the IEEE 57 standard. The research [20, 21] used an IEEE 57 bus system and an optimization technique called Moth Flame.

2. Moth flame optimisation

This is a method of optimisation with roots in the natural world. The algorithm's design was inspired by the moths' method of navigating at night. The moths fly at a steady angle towards the moon. Moths often fly in spiral patterns around lights. The multi-objective function's solution is assumed to be represented by the moths. One of the parameters of the issue is the spatial distribution of the moths. The following is a summary of the mathematical models of moth behavior: In light of these constraints, we describe the logarithmic spiral used by the MFO method flow diagram shown in Figure 1, as where S is the spiral function, M_i is the i-th moth, and F_j stands for the j-th flame.

$$M_i = S(M_i,\ F_i) \tag{1}$$

$$S(M_i,\ F_i) = D_i.e^{bt}.\cos(2\pi t) + F_j \tag{2}$$

D_i is the distance between the i-th moth and the j-th flame, b is a constant used to define the shape of the logarithmic spiral, and t is a random number in the interval $[-1, 1]$.

$$D_i = |F_j - M_i| \tag{3}$$

where M_i is the i-th moth for the j-th flame and D_i is the distance between them.

3. Proposed methodology

3.1 *Multi objective function*

Minimizing a multi-objective function that includes the following research goals is being done.

Objective 1- Negative Social Welfare:

Increasing the demand side price while decreasing the production side cost maximizes social welfare. The term "social welfare" refers to the net benefit to society as opposed to the net benefit to either consumers or sellers. Since this function minimizes a negative value, it maximizes social welfare.

$$NSW = \sum_{i=1}^{NG} C_i(P_{Gi}) - \sum_{j=1}^{ND} B_j(P_{Dj}) \tag{4}$$

$$C(p_g) = \sum_{i=1}^{n} a_{gi} P_{gi}^2 + b_{gi} P_{gi} + c_{gi} \tag{5}$$

$$B(p_d) = \sum_{i=1}^{n} a_{di} P_{di}^2 + b_{di} P_{di} + c_{di} \tag{6}$$

Objective 2- Minimization of Power Loss:

$$F_2 = \sum_{k=1}^{NT} G_{k(i,\ j)} \left[V_i^2 + V_j^2 - 2V_i V_j \cos\left(\delta_{ij}\right) \right] \tag{7}$$

where, V_i, V_j = i, j voltage in p.u.

Objective 3- Voltage deviation minimization:

A good voltage profile can only be achieved by carefully maintaining the voltages and minimizing the voltage collapse that causes the huge voltage spikes.

The voltage deviation reduction goal function is:

$$F_3 = \sum_{i=1}^{N_B} \| V_m - 1 \| \tag{8}$$

Voltage at bus m and number of busses are indicated by V_m and N_b

Constraints:

$$\sum_{i=1}^{NG} P_{Gi} + WP - P_{LOSS} - P_L = 0 \tag{9}$$

$$P_{LOSS} = \sum_{j=1}^{N_{TL}} G_j [|V_i|^2 + |V_j|^2 - 2|V_i||V_j| \cos(\delta_i - \delta_j)] \tag{10}$$

$$P_i - \sum_{k=1}^{N_b} |V_i V_k V_{ik}| \cos(\theta_{ik} - \delta_i + \delta_k) = 0 \tag{11}$$

$$Q_i - \sum_{k=1}^{N_b} |V_i V_k V_{ik}| \sin(\theta_{ik} - \delta_i + \delta_k) = 0 \tag{12}$$

Inequality Constraints

$$V_i^{min} \leq V_i \leq V_i^{max} \tag{13}$$

$$\phi_i^{min} \leq \phi_i \leq \phi_i^{max} \tag{14}$$

$$TL_1 \leq TL_1^{max} \tag{15}$$

$$P_{Gi}^{min} \leq P_{Gi} \leq P_{Gi}^{max} \tag{16}$$

$$Q_{Gi}^{min} \leq Q_{Gi} \leq Q_{Gi}^{max} \tag{17}$$

$$K_{TCSC}^{min} \leq K_{TCSC} \leq K_{TCSC}^{max} \tag{18}$$

3.2 *Proposed amalgamated severity index*

Combining the line Voltage stability indicator with the line power flow congestion factor is offered as the basis for TCSC placement.

$$ASI_{lm} = w_1 \times LUF_{lm} + w_2 \times FVSI_{lm} \tag{19}$$

where,

$$w_1 + w_2 = 1 \tag{20}$$

The two indices for line lm's weighting factors are w_1 and w_2. Both indices have been given equal consideration in our analysis.

Transmission line congestion is quantified by a metric called the line utilization factor (21) (LUF).

$$LUF_{ij} = \frac{MVA_{ij}}{MVA_{ijmax}} \tag{21}$$

where is The line's line utilisation factor (*LUF*) in relation to buses *i* and *j*

The *MVA* rating of the line connecting nodes *i* and *j* is MVA_{ij} (max).

MVA_{ij} is the line's actual *MVA* rating between nodes *i* and *j*.

To assess line congestion, use the Line Utilization Factor.

The following equation (22) calculates the line-based Fast Voltage Stability Index (*FVSI*).

$$FVSI_{ij} = \frac{4Z^2 Q_j}{V_i^2 X} \tag{22}$$

where Z represents line impedance.

Q_j is the reactive power at bus j , and X is the line reactance.

V_i denotes the bus i voltage magnitude.

An *FVSI* shows the load's stable operating range. Line stability diminishes with high *FVSI*. *FVSI* higher than signals system instability.

3.3 *Stepwise procedure*

The following steps solve the multi-objective OPF problem:

(1) Solar and wind power units are installed on selected transmission system buses.

(2) The OPF is executed for the multi-objective function.

(3) The amalgamated severity index is used to determine the placement of TCSC.

(4) The OPF and TCSC optimization are done for the multi-objective function.

(5) Performance of contingency analysis tests system robustness.

4. Results

Figure 1 depicts an IEEE 57 bus system with 80 lines of transmission, six PV nodes, one slack bus, and the remaining load nodes. Currently, TCSCs are only being installed on load buses. Solar and wind power replace the final two remaining thermal generators at bus 9 and bus 12.

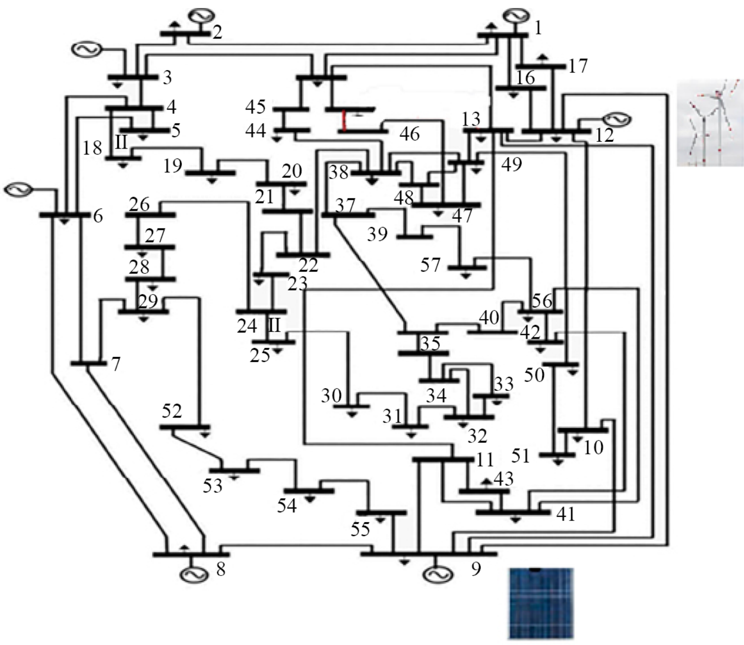

Figure 1. 57 bus transmission system

The 57-bus system has two lines that are being analyzed for potential problems: lines 7-8 and 11-41. Table 1 compares the outcomes of running OPF on single objective functions and then running it on multi-goal functions during the line 7-8 if/then block. A Negative Social Welfare objective (OF_1), a Voltage Deviation objective (OF_2), an Active Power Loss objective (OF_3), and a Multi-objective Optimization objective (OF_4). It is shown that the multi-objective function achieves relatively optimal parameters of all four goals, with OF_1 achieving the minimal value of NSW, OF_2 achieving the minimum value of voltage variation 4.96 p.u., and OF_3 attaining the least value of active power loss of 24.7497 MW. In this analysis, each goal was given equal weight, although that might be adjusted as needed.

Table 1. Different goal functions and optimal power flows for renewable energy sources without TCSC at lines 7-8

S.No	Parameter		OF_1	OF_2	OF_3	OF_4
1	Real power generation (MW)	P_{G1}	130.2112	109.7605)	191.6535	138.2444
		P_{G2}	100.0000	100.0000	1.3777	100.0000
		P_{G3}	41.8954	140.0000	140.0000	47.9197
		P_{G6}	9.0663	100.0000	100.0000	33.1509
		P_{G8}	410.1298	234.3875	250.4328	369.2346
		P_{Gs}	180.0000	180.0000	180.0000	180.0000
		P_{Gw}	350.0000	350.0000	350.0000	350.0000
2	Total Active power generation (MW)		1,221.3027	1,214.148	1,213.464	1,218.5496
3	Total real power generation cost ($ /hr)		21,606	25,837	25,837	21,728
4	Active power Loss (MW)		25.5027	18.3480	17.6639	22.7497
5	Valve point effect($ /hr)		21,662	25,879	25,875	21,796
6	Voltage deviation (p.u.)		5.0913	4.9587	4.9625	5.0569
7	CE(ton/hr)		0.7136	0.4074	0.5250	0.6188
8	FPL		4,462.8	4,462.8	4,462.8	4,462.8
9	FPG		21,606	25,837	25,837	21,728
10	NSW		17,143.2	21,374.2	21,374.2	17,265.2
11	Objective function		1.7143e + 04	4.9587	17.6639	2.0046e + 04

Table 2. Power flow optimizations for renewable energy sources without TCSC and objectives functions at line 11-41

S.No	Parameter		OF_1	OF_2	OF_3	OF_4
1	Real power generation (MW)	P_{G1}	127.8902	124.7857	118.2606	134.7974
		P_{G2}	100.0000	100.0000	100.0000	100.0000
		P_{G3}	40.6374	140.0000	97.3383	45.4064
		P_{G6}	1.0867	28.3348	100.0000	12.9954
		P_{G8}	417.8161	292.0607	268.5176	393.3626
		P_{Gs}	180.0000	180.0000	180.0000	180.0000
		P_{Gw}	350.0000	350.0000	350.0000	350.0000
2	Total Active power generation (MW)		1,217.4304	1,215.1812	1,214.1165	1,216.5618
3	Total real power generation cost ($/hr)		21,430	24,453	23,837	21,470
4	Active power Loss (MW)		21.6304	19.3812	18.3166	20.7619
5	Valve point effect ($/hr)		21,484	24,514	23,897	21,519
6	Voltage deviation (p.u.)		5.4634	5.3751	5.4021	5.4500
7	CE (ton/hr)		0.7325	0.4864	0.4377	0.6738
8	FPL		4,462.8	4,462.8	4,462.8	4,462.8
9	FPG		21,430	24,453	23,837	21,470
10	NSW		16,967.2	19,990.2	19,374.2	17,007.2
11	Objective function		1.6967e + 04	5.3751	18.3166	1.9628e + 04

Similar findings have been observed throughout line 11-41 contingency in Table 2. Parameter comparison reveals, however, that the hazard posed by the scenario at line 7-8 is more serious. TCSC has been positioned between line 41-43 based on Severity Index values for all lines of IEEE 57 bus system in Table 3. Figure 2 shows the difference between the Amalgamated Severity Index (ASI) with and without TCSC. It has been noted that the installation of TCSC has decreased the ASI of the severely affected lines. Similar comparisons may be made between the LUF and FVSI values at each of the 57 bus system's transmission lines (Figures 3 and 4).

Table 3. Values on the severity index lines of IEEE 57 Bus Lines

RANK	Line connected		FVSI	LUF	ASI
	SEB	REB			
1	11	41	1.0996	0.5408	0.6331
2	7	8	0.5003	0.4859	0.3502
3	41	43	0.0026	0.4332	0.273
4	8	9	0.0026	0.4228	0.2277
5	12	13	0.1555	0.2968	0.2261
6	44	45	0.2005	0.2342	0.2174
7	1	15	0.0763	0.3466	0.2114
8	13	49	0.2051	0.2128	0.2092
9	7	29	0.0608	0.3334	0.1971
10	15	45	0.1113	0.2562	0.1838
11	13	14	0.0614	0.2776	0.1695
12	13	15	0.0912	0.238	0.1646
13	1	2	0.0408	0.2784	0.1596
14	9	11	0.0641	0.2496	0.1568
15	1	15	0.1037	0.2004	0.1521
16	2	3	0.0638	0.2375	0.1507
17	6	8	0.05	0.2446	0.1473
18	14	46	0.0776	0.2167	0.1471
19	1	17	0.0261	0.267	0.1465
20	46	47	0.0785	0.2123	0.1454

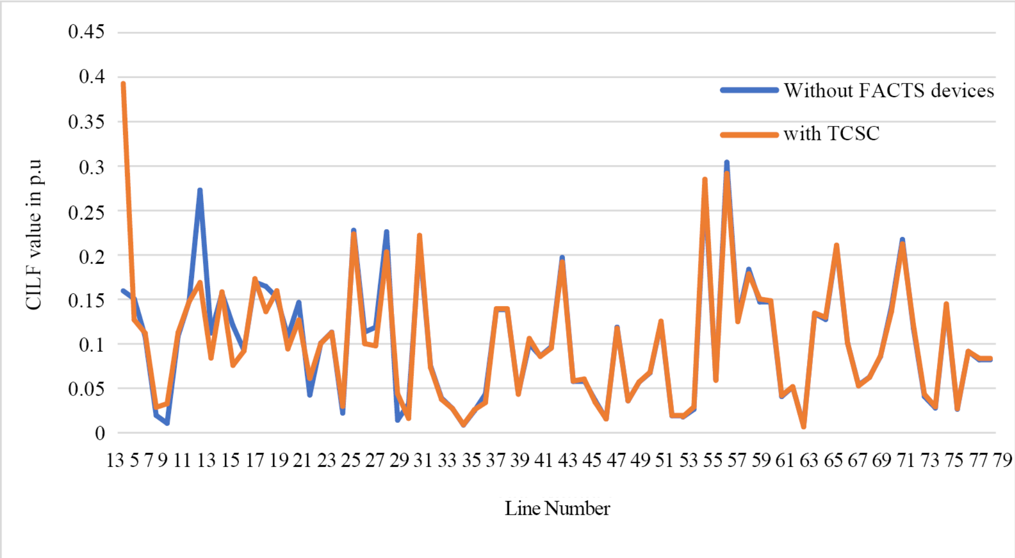

Figure 2. Difference of ASI with and without TCSC

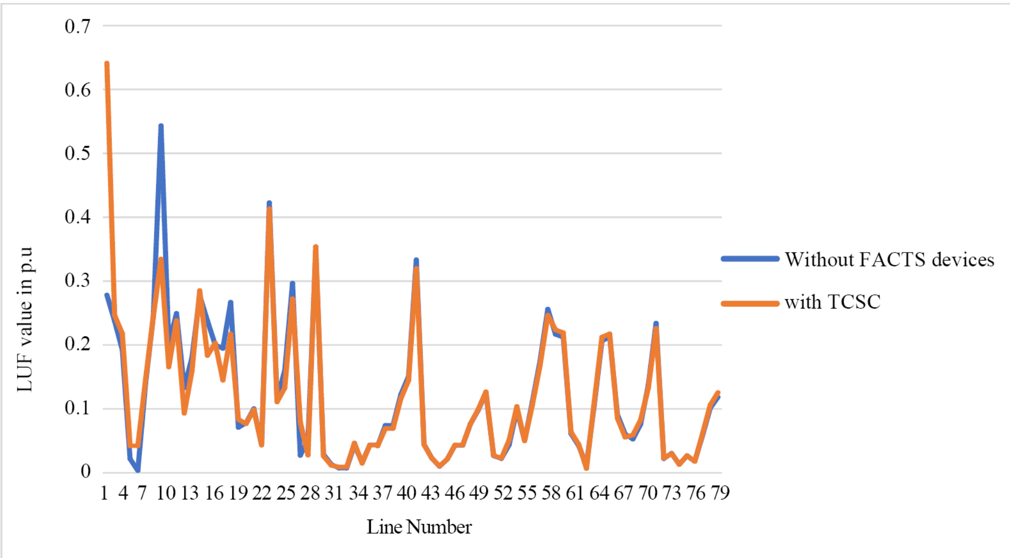

Figure 3. Study of LUF with and without TCSC

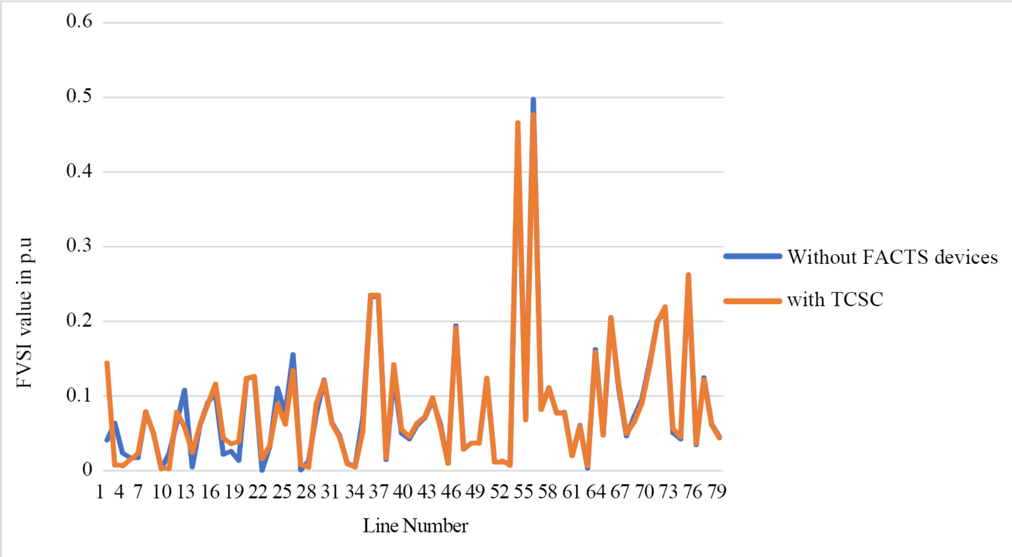

Figure 4. Study of FVSI with and without TCSC

The 57-bus system's power flow is optimized once the TCSC is positioned and tuned for maximum efficiency. Table 3 shows that for the line 11-41 scenario, the power loss in the system decreases from 20.76 MW to 19.4761 MW. With the line 7-8 backup plan in place, system power loss drops from 22.75 MW to 21.73 MW (Table 4).

Table 4. Optimal power flows for various objective functions with contingency at line 11- 41 and renewable energy sources with TCSC

S.No	Parameter		OF_1	OF_2	OF_3	OF_4
1	Real power generation (MW)	P_{G1}	132.4001	195.9086	172.8360	141.5272
		P_{G2}	17.8836	100.0000	0.0219	64.5819
		P_{G3}	40.6892	0.2946	84.8188	44.1377
		P_{G6}	0.2090	94.6564	115.6291	4.8902
		P_{G8}	415.9399	232.3124	229.1141	350.1391
		P_{Gs}	200.0000	181.6454	200.0000	200.0000
		P_{Gw}	410.0000	410.0000	410.0000	410.0000
2	Total Active power generation (MW)		1,217.1218	1,214.8174	1,212.4199	1,215.2761
3	Total real power generation cost ($/hr)		18,224	21,626	21,078	18,403
4	Active power Loss (MW)		21.3217	19.0175	16.6198	19.4761
5	Valve point effect ($/hr)		18,277	21,659	21,105	18,459
6	Voltage deviation (p.u.)		5.5700	5.5243	5.5303	5.5415
7	CE (ton/hr)		0.6933	0.4649	0.4217	0.5450
8	P_{tcsc} (p.u)		0.2457	0.2324	0.2351	0.2408
9	Q_{tcsc} (p.u)		0.5156	0.5156	0.5156	0.5154
10	X_{tcsc} (p.u)		0.2132	0.1902	0.1662	0.1948
11	FPL		4,462.8	4,462.8	4,462.8	4,462.8
12	FPG		18,224	21,626	21,078	18,403
13	NSW		13,761.2	17,163.2	16,615.2	13,940.2
14	Objective function		1.3761e + 04	5.5243	16.6198	1.6441e + 04

Table 5. Optimal power flows for various objective functions with contingency at line 7-8 and renewable energy sources with TCSC

S.No	Parameter		OF_1	OF_2	OF_3	OF_4
1	Real power generation (MW)	P_{G1}	112.5234	174.3543	176.0608	139.4134
		P_{G2}	100.0000	100.0000	0.0057	39.7618
		P_{G3}	36.2526	0.0000	84.9416	46.9948
		P_{G6}	0.0005	200.0000	151.5579	32.0321
		P_{G8}	361.3731	129.6122	189.1001	349.3274
		P_{Gs}	200.0000	200.0000	200.0000	200.0000
		P_{Gw}	410.0000	410.0000	410.0000	410.0000
2	Total Active power generation (MW)		1,220.1496	1,213.9665	1,211.6661	1,217.5295
3	Total real power generation cost ($/hr)		18,615	25,009	22,462	18,575
4	Active power Loss (MW)		24.3496	18.1665	15.8661	21.7296
5	Valve point effect ($/hr)		18,666	25,050	22,496	18,650
6	Voltage deviation (p.u.)		5.0670	4.9838	4.9908	5.0507
7	CE (ton/hr)		0.5571	0.4555	0.4195	0.5341
8	P_{tcsc} (p.u)		0.1766	0.1613	0.1651	0.1760
9	Q_{tcsc} (p.u)		0.2888	0.2898	0.2894	0.2887
10	X_{tcsc} (p.u)		0.2435	0.1817	0.1587	0.2173
11	FPL		4,462.8	4,462.8	4,462.8	4,462.8
12	FPG		18,615	25,009	22,462	18,575
13	NSW		14,152.2	20,546.2	17,999.2	14,112.2
14	Objective function		1.4152e + 04	4.9838	15.8661	1.6790e + 04

The system voltage curve with and without FACTS devices is shown in Figure 5. Figure 6 compares multi-objective function convergence without and with TCSC. Figure 7 shows negative social welfare with and without TCSC in various system setups.

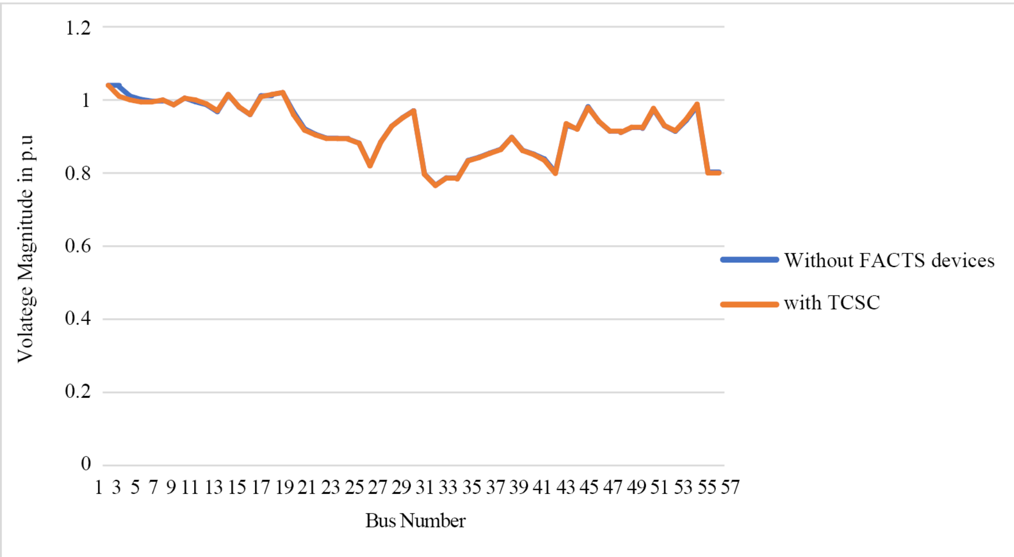

Figure 5. Multi-objective function voltage outline

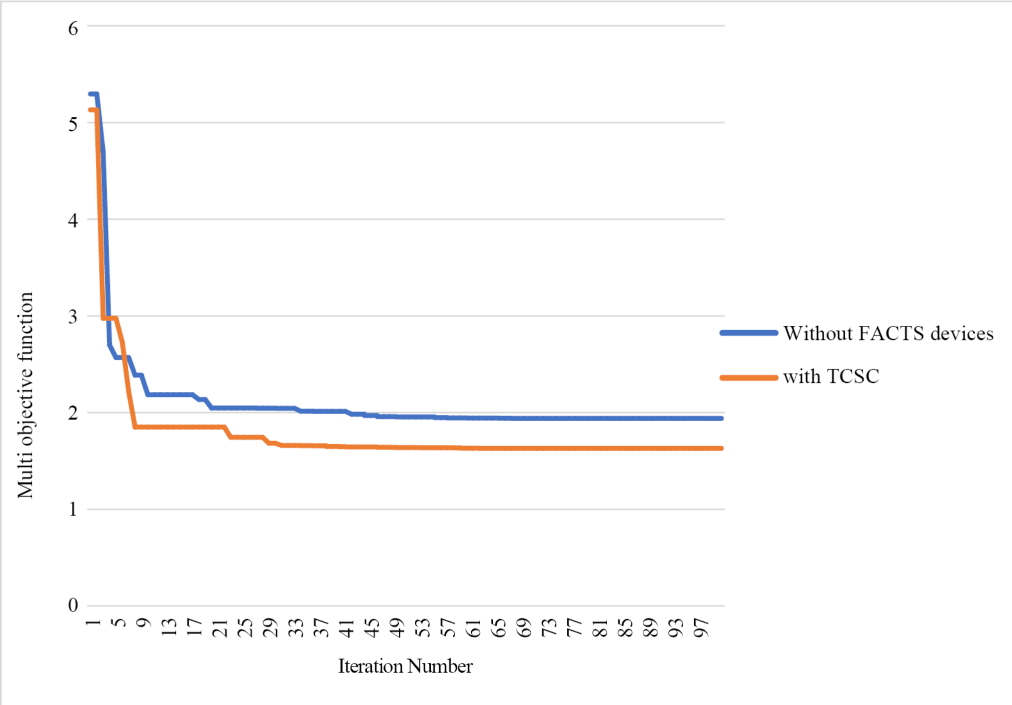

Figure 6. Multi-objective convergence

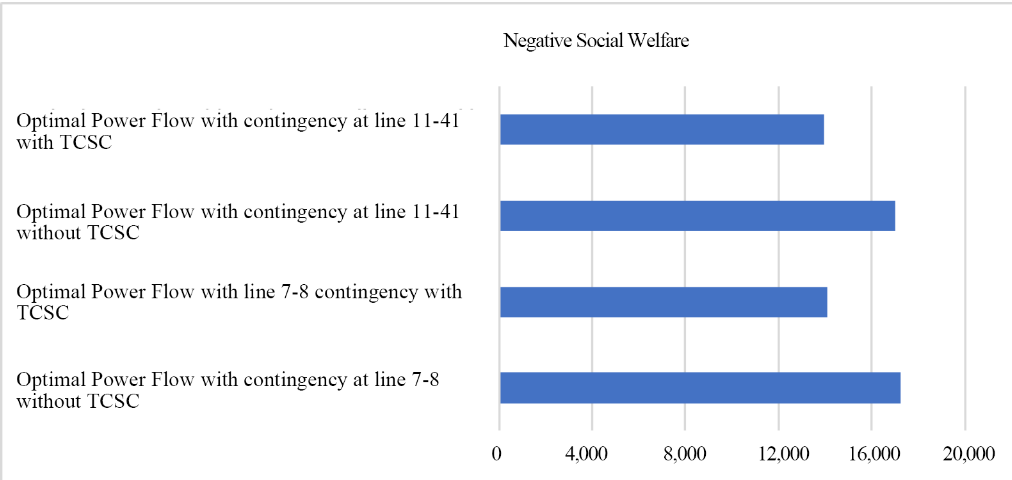

Figure 7. Negative social welfare with and without TCSC

5. Conclusions

Attracting industrial and foreign investment requires a reliable electricity grid. FACTS devices may be used in combination with renewable energy sources, which are already a potential alternative to conventional power systems, to boost the stability and dependability of the present power systems.

• The OPF enhances power flow capacity when renewable production is present.

• Optimal TCSC tuning and placement enhance system efficiency.

• TCSC deployment in the intended area leads to an 18% increase in social welfare.
• Moth Flame optimization is an effective approach for multi-objective problems.
• TCSC is a cost-effective alternative to conventional FACTS devices.

Conflict of interest

The author declares there is no conflict of interest at any point with reference to research findings.

References

[1] Lawal MO, Komolafe O, Ajewole TO. Power-flow-tracing-based congestion management in hydro-thermal optimal power flow algorithm. *Journal of Modern Power Systems and Clean Energy*. 2019; 7(3): 538-548.

[2] Batra I, Ghosh S. A novel approach of congestion management in deregulated power system using an advanced and intelligently trained twin extremity chaotic map adaptive particle swarm optimization algorithm. *Arabian Journal for Science and Engineering*. 2018; 44(10): 6861-6886.

[3] Teeparthi K, Kumar DMV. Multi-objective hybrid PSO-APO algorithm based security constrained optimal power flow with wind and thermal generators. *Engineering Science and Technology-An International Journal*. 2017; 20(2): 411-426.

[4] Ahmad AlA, Sirjani R. Optimal placement and sizing of multi-type FACTS devices in power systems using metaheuristic optimisation techniques: An updated review. *Ain Shams Engineering Journal*. 2020; 11(3): 611-628.

[5] Visakha K, Thukaram D, Jenkins L. Application of UPFC for system security improvement under normal and network contingencies. *Electric Power Systems Research*. 2004; 70(1): 46-55.

[6] Hayajneh A, Nusair K, Alasali F, Holderbaum W. Optimal placeent of FACTS devices and power-flow solutions for a power network system integrated with stochastic renewable energy resources using metaheuristic optimization techniques. *International Journal of Energy Research*. 2021; 21(3): 1-24.

[7] Dawn S, Tiwari P, Goswami AK. An approach for long term economic operations of com-petitive power market by optimal combined scheduling of wind turbines and FACTS controllers. *Energy*. 2019; 181(3): 709-723.

[8] Rui M, Xuan L, Yang L, Xia W, Fei J. Multi-objective dynamic optimal power flow of wind integrated power systems considering demand response. *CSEE Journal of Power and Energy Systems*. 2019; 5(4): 466-473.

[9] Velayutham U, Ponnusamy L, Venugopal G. Minimization of cost and congestion management using interline power flow controller. *COMPEL-The International Journal for Computation and Mathematics in Electrical and Electronic Engineering*. 2016; 35(5): 1495-1512.

[10] Daram SB, Venkataramu PS, Nagaraj MS. Performance index based contingency ranking under line outage condition incorporating IPFC. *International Conference on Electrical, Electronics, and Optimization Techniques (ICEEOT)*. Chennai, India: IEEE; 2016.

[11] Yang, XS. Firefly algorithm, lévy flights and global optimization. In: Bramer M, Ellis R, Petridis M. (eds.) *Research and Development in Intelligent Systems XXVI*. London: Springer; 2010. p.209-218. Available from: doi:10.1007/978-1-84882-983-1_15.

[12] Upadhyay A, Kumar GVN. Line utilisation factor-based optimal allocation of IPFC and sizing using firefly algorithm for congestion management. *Advances in Electrical and Electronic*. 2016; 14(2): 1-8.

[13] Kumar GN, Kalavathi MS. Cat swarm optimization for optimal placement of multiple UPFC's in voltage stability en-hancement under contingency. *Electrical Power and Energy Systems*. 2014; 57: 97-104. Available from: doi:10.1016/j.ijepes.2013.11.050.

[14] Verma R, Rathore A. Optimal placement of facts device considering voltage stability and losses using teaching learning based optimization. *Journal of The Institution of Engineers (India): Series B*. 2021; 102: 771-776. Available from: doi:10.1007/s40031-021-00582-w.

[15] Adetokun BB, Muriithi CM. Application and control of flexible alternating current transmission system devices for voltage stability enhancement of renewable-integrated power grid: A comprehensive review. *Heliyon*. 2021; 7(3): e06461.

[16] Aghdam FH, Ghaemi S, Safari A, Farrokhifar M. Profit-based evaluation of optimal FACTS devices planning for the large consumers and TRANSCO considering uncertainty. *International Transactions on Electrical Energy Systems*. 2021; 31(4): e12828.

[17] Oyekanmi WA, Radman G, Babalola AA, Ajewole TO. Power system simulation and contingency ranking using load bus voltage index. *Engineering Science and Technology-An International Journal*. Abuja, Nigeria: IEEE; 2014.

[18] Ghaemi S, Aghdam FH, Safari A, Farrokhifar M. Stochastic economic analysis of FACTS devices on contingent transmission networks using hybrid biogeography-based optimization. *Electrical Engineering*. 2019; 101: 829-843. Available from: doi:10.1007/s00202-019-00825-6.

[19] Biswas PP, Arora P, Mallipeddi R, Suganthan PN, Panigrahi BK. Optimal placement and sizing of FACTS devices for optimal power flow in a wind power integrated electrical network. *Neural Computing and Applications*. 2020; 33: 6753-6774. Available from: doi:10.1007/s00521-020-05453-x.

[20] Mirjalili S. Moth-flame optimization algorithm: A novel nature-inspired heuristic paradigm. *Knowledge-Based Systems*. 2015; 89: 228-249. Available from: doi:10.1016/j.knosys.2015.07.006.

[21] Li Y, Zhu XY, Liu JS. An improved moth-flame optimization algorithm for engineering problems. *Symmetry*. 2020; 12(8): 1234.